THE STRUCTURE AND ENERGY OF CROSS-TIE DOMAIN WALLS

By R. Kosiński

Institute of Physics, Technical University of Warsaw*

(Received July 15, 1976; final version received October 26, 1976)

Two models of the cross-tie wall in thin ferromagnetic films are given. For the description of the Bloch-type segments of the main wall in the first model, the previously published models of the cross and the circular Bloch lines are used. In the second model, the simple model of the low-angle Bloch wall was used to describe these fragment of the main wall. For both models the surface energy density σ as a function of film thickness D is obtained. These functions lie below the functions $\sigma(D)$ obtained in previous papers, in all ranges of film thickness (0 Å $< D <$ 2000 Å) for the first model and for $D \gtrsim 550$ Å for the second model. The distance s between side walls as a function of D is, for the first model, in qualitative agreement with experimental data.

1. Introduction

The cross-tie walls in this ferromagnetic films were investigated by many authors [1, 2]. Such a wall has a three dimensional structure and therefore the exact evaluation of its energy is very difficult [2]. In previous papers some crude approximations to evaluate its energy were made [3–7].

The most recent model of the cross-tie walls was proposed by Minnaja [6]. However, the distance between side walls in that model tends to zero for very thick films, and there are no differences in expressions for the energies of the circular and cross Bloch lines, which are considered as modified fragments of the Bloch walls. On the other hand, it is known from the experimental data [3, 8, 9], that the distance between side walls increases for increasing D if $D > D_0$, contrary to Minnja's result (D is the thickness of the film).

In this paper two new models of the cross-tie walls are presented. In both models we used a magnetization distribution similar to that used by Minnaja [6]. The main difference between the models presented here and Minnaja's is in the different description of the Bloch-type segments in the main wall. In the first model we used the model of the cross Bloch lines given by Bäurich [11] and the model of circular Bloch lines given by Feldkeller-

* Address: Instytut Fizyki, Politechnika Warszawska, Koszykowa 75, 00-662 Warszawa, Poland.

-Thomas [10]. In the second model we describe the Bloch-type segments in the main wall with the help of Middlehoek's model of the low angle Bloch wall [12]. After the numerical minimization of the expression for the energy density for both models we obtained the behaviour of the main cross-tie wall parameters in the function for film thickness.

2. *Model I*

We assume the periodic structure of the wall as presented on Fig. 1. The easy axis of the film lies in the film plane. The cross-tie wall in our model consists of the main wall (II), which has the alternating orientation of magnetization, and the side walls (III). Both of them are Néel walls. The main wall is divided into segments by the circular (V) and the

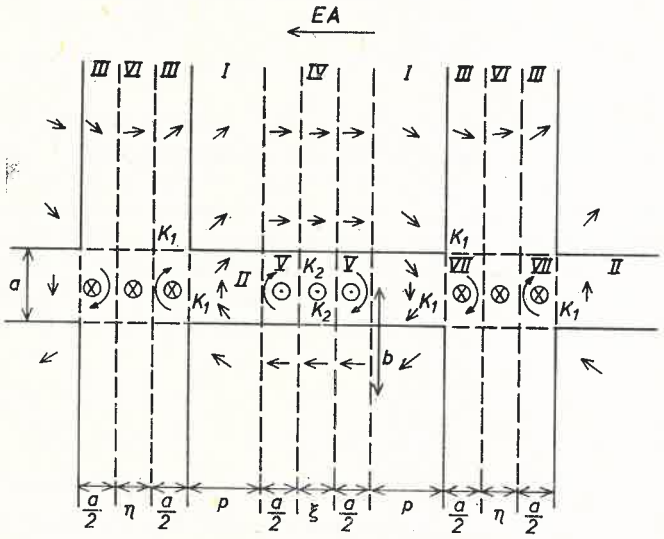

Fig. 1. The structure of the first model

cross Bloch lines (VII). The Bloch lines are divided at their mid-points into two equal parts and segments of the Bloch walls are set between them. These segments (IV, VI) have the lengths η ans ξ for cross and circular Bloch lines, respectively. Oustide the main and side walls the magnetization vector $\vec{M}$ is assumed to be tangent to the concentric circles (I), the common centre of which lies on the straight line perpendicular to the main wall at a distance b from it. The character of the direction cosines is such, that on the surfaces dividing elements (I, II, etc.) of the wall the magnetization is continuous. The discontinuities appear only in the main wall on the surfaces K_1 and K_2, which are shown on Fig. 1. The discontinuities, being small, should not cause any additional significant error in the calculations. It is worth noticing that for increasing b the effective lengths of the side walls also increase. For $\eta = \xi = 0$ the present model is similar to the model presented by Minnaja.

The total energy per unit area of the wall is the sum of the anisotropy exchange and demagnetization energies. The expressions for different types of energies were obtained

after intergrating over different segments of the wall. The density of the energy of uniaxial anisotropy E_K is given by the general formula (in all formulas the indices of E correspond to those used on Fig. 1).

$$E_K = K \sin^2 \alpha, \tag{1}$$

where K is anisotropy constant, α — the angle between $\vec{M}$ and EA. For our model we have

$$E_{KI} = 2K\left[(p^2+t^2)\,\mathrm{arctg}\,\frac{p}{t} - pt\right], \tag{2}$$

where $t = b+a/2$

$$E_{KII} = K\left(ap - \tfrac{1}{3}\,at\,\mathrm{arctg}\,\frac{p}{t}\right), \tag{3}$$

$$E_{KIII} = 2K\,\frac{ap}{3}\,\mathrm{arctg}\,\frac{p}{t}\,. \tag{4}$$

The initial formula for the exchange energy used for our model is given by the expression

$$E_{ex} = A[(\nabla\alpha_1)^2+(\nabla\alpha_2)^2+(\nabla\alpha_3)^2]. \tag{5}$$

(A — denotes the exchange constant, $\alpha_i (i = 1, 2, 3)$ the direction cosines of $\vec{M}$.) From this we obtained the exchange energies expressed by nonelementary integrals

$$E_{exI} = 2A\int_0^{p/t} \frac{1}{w}\,\mathrm{arctg}\,w\,dw, \tag{6}$$

$$E_{exII} = A\left[\frac{a}{3}\left(\frac{p}{p^2+t^2} + \frac{1}{t}\,\mathrm{arctg}\,\frac{p}{t}\right) + \frac{8t}{a}\int_0^{p/t} \mathrm{arctg}^2\,\frac{1}{w}\,dw\right], \tag{7}$$

$$E_{exIII} = A\left[\frac{a}{6p}\left(\mathrm{arctg}\,\frac{p}{t} - \frac{pt}{p^2+t^2}\right) + \frac{4p}{a}\int_{t/p}^{\infty} \mathrm{arctg}^2\,\frac{1}{w}\,dw\right]. \tag{8}$$

The magnetostatic energies of the main walls and the side walls are evaluated assuming that they have the shape of elliptical cylinders. We used the demagnetization factor for an elliptical cylinder:

$$N = 4\pi D/(a+D) \tag{9}$$

(D, a — denotes the ellipse axis.) Thus the magnetostatic energy is given by:

$$E_M = \tfrac{1}{2}\,NM_{eff}, \tag{10}$$

where M_{eff} is the effective magnetization of the cylinder which is surrounded by the areas denoted by I of the wall. M_{eff} is the function of the distance from the areas I of the wall and the distance from the Bloch lines areas. For the main wall we have

$$M_{\text{eff}} = M_{\text{eff}}(x, y) = M_s \cos \alpha(x, y) - M_s \cos \alpha\left(\frac{a}{2}, y\right). \tag{10a}$$

(The centre of the cartesian coordinate system lies on the surface which separates the areas II and V of the wall, see Fig. 1, in the middle of the main wall. The axis x is parallel to the side walls, α is the angle between $\vec{M}_s$ and the x axis). We obtain the following expression for the magnetostatic energy:

$$E_{M\text{II}} = \frac{4\pi M_s^2 D}{a+D}\left[2a(p+t) - \tfrac{4}{3} at \operatorname{arctg}\frac{p}{t} - 2a\sqrt{p^2+t^2} + \frac{at}{3} - \frac{at^2}{3\sqrt{p^2+t^2}}\right]. \tag{11}$$

Analogously for the side walls we obtain:

$$E_{M\text{III}} = \frac{4\pi M_s^2 D}{a+D}\left[2a\sqrt{p^2+t^2} + \frac{ap^2}{3\sqrt{p^2+t^2}} - 2at - \tfrac{1}{3} ap \operatorname{arctg}\frac{p}{t}\right]. \tag{12}$$

(The centre of the cartesian coordinate system lies now in the centre of the cross Bloch line with the x axis parallel to the main wall, α is the angle between $\vec{M}_s$ and x axis, see Fig. 1).

The energy of Bloch lines E_L is evaluated following the method of Feldkeller and Thomas [10] for the circular Bloch lines (V). For ths cross Bloch lines (VII) the model of Bäurich [11] was used. The surface density of the energy for Bloch-type segments of the main wall (V), following Middlehoek's method [12] is:

$$\sigma_B = A\pi^2/a + \tfrac{1}{2} aK + \pi a^2 M_s^2/(a+D). \tag{13}$$

In our model we neglect the magnetostatic interactions between the different segments of the wall. We assume that the energy connected with these interactions and with the discontinuities of $\vec{M}$ on the surfaces K_1, K_2 is small in comparison with the other energy terms. The total energy per unit area of the cross-tie wall is

$$\sigma = (2p+\lambda)^{-1}(E_{K\text{I}} + E_{K\text{II}} + E_{K\text{III}} + E_{\text{exI}} + E_{\text{exII}} + E_{\text{exIII}}$$

$$+ E_{M\text{II}} + E_{M\text{III}} + E_L/a + \lambda\sigma_B)\ [\text{erg} \cdot \text{cm}^{-2}]. \tag{14}$$

We use here the same notations as in formulas (1) — (14). We also assumed $2(a+p)+\lambda \approx 2p+\lambda$. For numerical evaluation the following values of material constants were used: $M_s = 800$ Gs, $A = 10^{-6}$ ergcm^{-1}, $K = 10^3$ ergcm^3.

The numerical minimization of (14) with respect to a, p, b, λ, for the film thickness $D \in [50; 2000]$ Å was made with the help of the CYBER-72 C.D.C. computer system. For computing the non-elementary integrals in (6) — (8) we used a separate subroutine. The energies of the Bloch lines were introduced into the program as a $[2 \times 60]$ matrix for

all film thicknesses from 50 Å to 3000 Å. In order to minimize (14) the method of steepest descent was used for each assumed film thickness.

Our most important numerical results are shown on Figs. 3 — 7.

3. *Model II*

We assume the periodic structure as presented on Fig. 2. The easy axis of the film lies in the film plane. The cross-tie wall in our model consists of the main wall (II), which has the alternating orientation of magnetization and of the side walls (III). Both of them

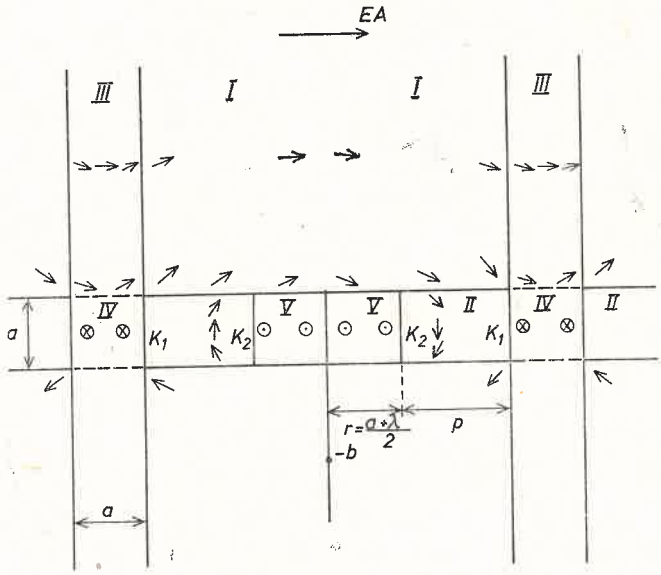

Fig. 2. The structure of the second model

are Néel walls. The main wall is divided into sections by the segments of the Bloch walls (V, IV) which represents the Bloch-type areas in the main wall. They have the lengths $r = \frac{1}{2}(a+\lambda)$ and a respectively for the segments in the centre of main wall (V) and for the segments lying at the intersection of the main and side walls (IV). Outside the main and side walls (I) the magnetization vector $\vec{M}$ is assumed to be tangent to the concentric circles, the common centre of which lies on a straight line perpendicular to the main wall at a distance b from it. The character of the direction cosines of $\vec{M}$ is such that on the surfaces dividing different elements (I, II, etc.) of the wall, including the Bloch segments, the magnetization is continuous. The discontinuities appear only in the main wall on the surfaces K_1, K_2, which are shown on Fig. 2. The discontinuities being small should not cause any additional significant error in the calculations. It is worth noticing that for r and p constant and increasing b the effective lengths of the side walls increase.

The total energy per unit surface of the wall is the sum of the anisotropy exchange and demagnetization energies for all fragments of the wall. After integrating over all

areas of the wall, we obtain for each of the the areas the energy of uniaxial anisotropy E_k. In all formulas the indices of E correspond to those used on Fig. 2.

$$E_{KI} = 2K[(p+r)^2+t^2]\,\mathrm{arctg}\,\frac{p+r}{t}, \tag{15}$$

where $r = \frac{1}{2}(a+\lambda)$; $t = b+a/2$,

$$E_{KII} = 2K\left[ap - \frac{at}{3}\left(\mathrm{arctg}\,\frac{r+p}{t} - \mathrm{arctg}\,\frac{r}{t}\right)\right], \tag{16}$$

$$E_{KIII} = 2Ka\,\frac{p+r}{3}\,\mathrm{arctg}\,\frac{p+r}{t}, \tag{17}$$

where K is the anisotropy constant.

The exchange energy is (A — exchange constant, α_1, α_2, α_3 — direction cosines of $\vec{M}$)

$$E_{ex} = A[(\nabla\alpha_1)^2+(\nabla\alpha_2)^2+(\nabla\alpha_3)^2]. \tag{18}$$

These above energies expressed by the non-elementary integrals are

$$E_{exI} = 4A\int_{r/t}^{\frac{r+p}{t}} \frac{1}{w}\,\mathrm{arctg}\,w\,dw, \tag{19}$$

$$E_{exII} = A\left[\frac{8t}{a}\int_{r/t}^{(r+p)/t} \mathrm{arctg}^2\,\frac{1}{w}\,dw + \frac{a}{3}\left(\frac{r+p}{(r+p)^2+t^2} - \frac{r}{r^2+t^2}\right)\right.$$
$$\left. + \frac{a}{3t}\left(\mathrm{arctg}\,\frac{p+r}{t} - \mathrm{arctg}\,\frac{r}{t}\right)\right], \tag{20}$$

$$E_{exIII} = A\left[\frac{4(r+p)}{a}\int_{t/(r+p)}^{\infty} \mathrm{arc\,tg}^2\,\frac{1}{w}\,dw + \frac{a}{6(r+p)}\left(\mathrm{arc\,tg}\,\frac{r+p}{t} - \frac{(r+p)t}{(r+p)^2+t^2}\right)\right]. \tag{21}$$

The demagnetization energy is evaluated assuming that the main wall and the side walls are in the shape of elliptical cylinders. The demagnetization factor for such cylinders is

$$N = 4\pi D/(a+D), \tag{22}$$

where a, D are the lengths of the ellipse axis. We also neglect the magnetostatic interactions for different segments of the wall. Thus we have

$$E_M = \tfrac{1}{2}\,NM_{eff}, \tag{23}$$

$$M_{eff} = M_{eff}(x, y) = M_s\cos\alpha(x, y) - M_s\cos\alpha\left(\frac{a}{2}, y\right). \tag{23a}$$

In the case of the main wall (see Fig. 2) the centre of the cartesian coordinate system lies between the side walls in the middle of the main wall with the x axis parallel to the side walls. In the case of the side walls the centre of the cartesian coordinate system lies in the middle of the cross Bloch line and the x axis is parallel to the main wall. In both cases α denotes the angle between $\vec{M}_s$ and x axis.

For the main wall we have

$$E_{M\text{II}} = \frac{4\pi M_s^2 D}{a+D}\left[2ap - \tfrac{4}{3}at\left(\operatorname{arc\,tg}\frac{r+p}{t} - \operatorname{arc\,tg}\frac{r}{t}\right) + 2a(\sqrt{r^2+t^2} - \sqrt{(r+p)^2+t^2}) + \frac{at^2}{3}(1/\sqrt{r^2+t^2} - 1/\sqrt{(r+p)^2+t^2})\right]. \tag{24}$$

For the side wall we have

$$E_{M\text{III}} = \frac{4\pi M_s^2 D}{a+D}\left[2a\sqrt{(r+p)^2+t^2} + \frac{a(r+p)^2}{3\sqrt{(r+p)^2+t^2}} - 2at - \tfrac{4}{3}a(r+p)\operatorname{arc\,tg}\frac{r+p}{t}\right]. \tag{25}$$

The energy of the Bloch segments is evaluated using a model of the Bloch wall in which the magnetization rotates through an angle which is less than 180° [12]. This angle varies along the main wall so that the magnetization vector is continuous on the surfaces which divide the areas I and II of the cross-tie wall. We obtain

$$E_{L\text{V}} = 2\sigma_B\left(b + \frac{a}{2}\right)\operatorname{arc\,tg}\frac{a+\lambda}{2b+a}, \tag{26}$$

$$E_{L\text{IV}} = a\sigma_B\left[1 - \frac{(p+\frac{1}{2}a+\frac{1}{2}\lambda)^2}{(p+\frac{1}{2}a+\frac{1}{2}\lambda)^2 + \left(b+\frac{a}{2}\right)^2}\right], \tag{27}$$

where σ_B is the density of the energy of the 180°-Bloch wall following Middlehoek [12]. We note that we used a distribution of magnetization similar to those used in [6]. The differences between the present model and those of Ref. [6] are included in various assumption concerning Bloch-type areas in the main wall of the cross-tie wall. In the current model which differs from the previous one in that the Bloch lines in the Bloch-type segments are not described separately. The total energy per unit area of the cross-tie wall is

$$\sigma = (2a+2p+\lambda)^{-1}(E_{K\text{I}} + E_{K\text{II}} + E_{K\text{III}} + E_{ex\text{I}} + E_{ex\text{II}} + E_{ex\text{III}} + E_{M\text{II}} + E_{M\text{III}} + E_{L\text{V}} + E_{L\text{IV}})\ [\text{erg}\cdot\text{cm}^{-2}], \tag{28}$$

where we used the same notation as in formulas (15) to (27). This expression was minimized with respect to a, p, b, λ for changing values of film thickness D from 50 Å to 2000 Å with the help of the CYBER 72 C.D.C. computer system. For computations we used the steepest descent method. The non-elementary integrals in (18) — (21) were computed with the help of a separate subroutine. We assumed the following values of material parameters: $K = 10^3$ ergcm^3, $M_s = 800$ Gs, $A = 10^{-6}$ ergcm^{-1}. The most important numerical results are shown on Figs. 3 — 6.

4. Results and discussion

The total energy density σ for the cross-tie wall as a function of tie film thickness D is shown on Fig. 3. For the first model, we note that the curve $\sigma(D)$ lies below the one obtained in the most recent model of the cross-tie wall [6] for the whole range of D. We

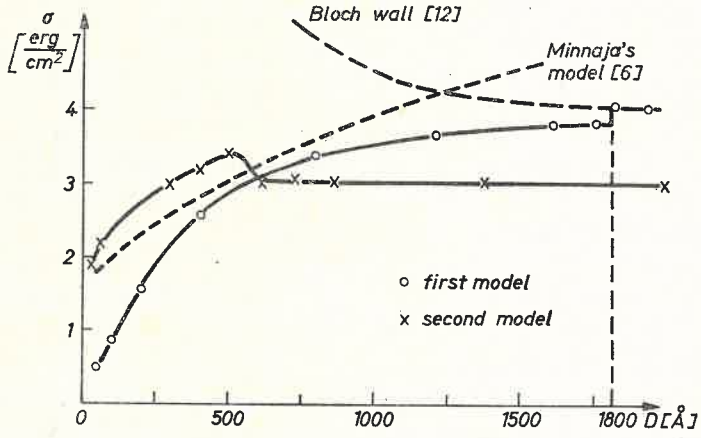

Fig. 3. The energy density σ as a function of film thickness D

believe this to be the most valuable result. For the second model, we obtained smaller value of the energy density than Minnaja [6] for $D \gtrsim 550$ Å.

The behaviour of the parameter $\lambda(D)$ (Fig. 4) shows the share of the Bloch type segments (IV, VI) in the main wall (II) as a function of D. It should seem that this share

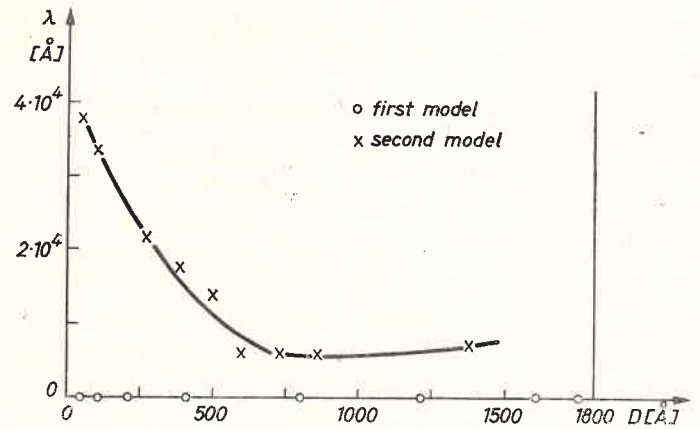

Fig. 4. The length of the Bloch type segments λ as a function of D

for large thicknesses should be larger as it causes the lowering of the magnetostatic energy in the main wall. The presence of Bloch type fragments in the main wall was observed experimentally by Feldkeller and Fuchs [8]. For our first model apart from Bloch lines

the behaviour of $\lambda(D)$ shows the lack Bloch segments in the main wall. At a thickness od $D = 1800$ Å λ increases to infinity. This means that the cross-tie wall changes into a Bloch wall — at this point there is a step on the $\sigma(D)$ curve. This fact seems to lack any physical meaning and should be caused by the used — for the description of Bloch type segments in the main wall — of an oversimplified model. For the second model, we notice that Bloch segments in the main wall can occur even in the thinnest films — this fact was not observed experimentally. Despite that the parameter λ — once introduced — allows for a theoretical analysis of the behaviour of the Bloch type segments using the above simple description of them.

One of the easiest to observe parameters of the cross-tie wall is the distance s between the side walls as a function of film thickness. In previous models [3–7] the functions $s(D)$ differ qualitatively from most of the experimental data [12–14]. The distance between

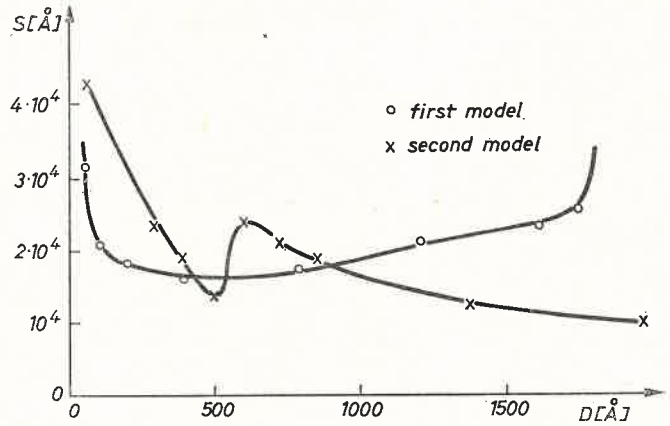

Fig. 5. The distance between side walls s as a function of film thickness D

side walls as a function of film thickness is shown on Fig. 5. For the first model the behaviour of the curve is in qualitative agreement with experimental data [12–14]: the distance between the side walls increases for films thinner than 400 Å and thicker than 1600 Å. For the second model we obtained that the distance s between the side walls decreases with increasing film thickness. Above 500 Å s increases and then decreases again for D over 650 Å contrary to the majority of the experimental data.

The effective lenght l of the side walls is given by the ratio p/b for the first model and by $(p+\frac{1}{2}a+\frac{1}{2}\lambda)/b$ for the second model. This parameter as a function of film thickness is shown on Fig. 6. We note in passing that the side walls are longer in the thinner films for the presented models. This has been confirmed by experimental observations [12–15].

The range of film thickness $D_1 < D < D_2$ for which the cross-tie wall energy is smaller than the energy of the Néel wall and of the Bloch wall should fall in the range of film thickness in which such walls are observed. The theoretical range depends on the Néel wall models and the Bloch wall models which are used for comparison with the cross-tie wall energy. For the simple one dimensional models of the Néel and Bloch walls [12]

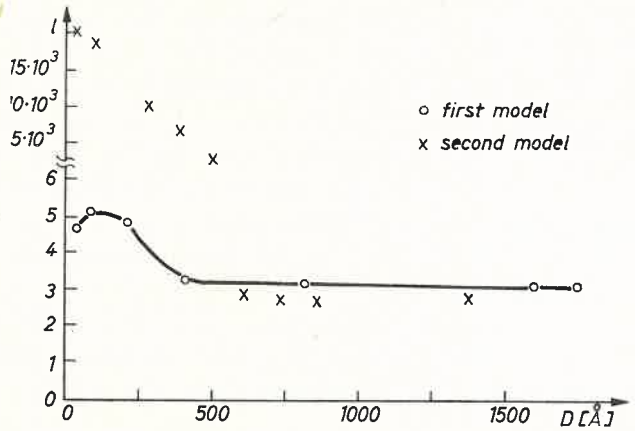

Fig. 6. Effective length of the side walls $l \sim p/b$ for the first model and $l \sim (p+\frac{1}{2}a+\frac{1}{2}\lambda)/b$ for the second model as function of film thickness D

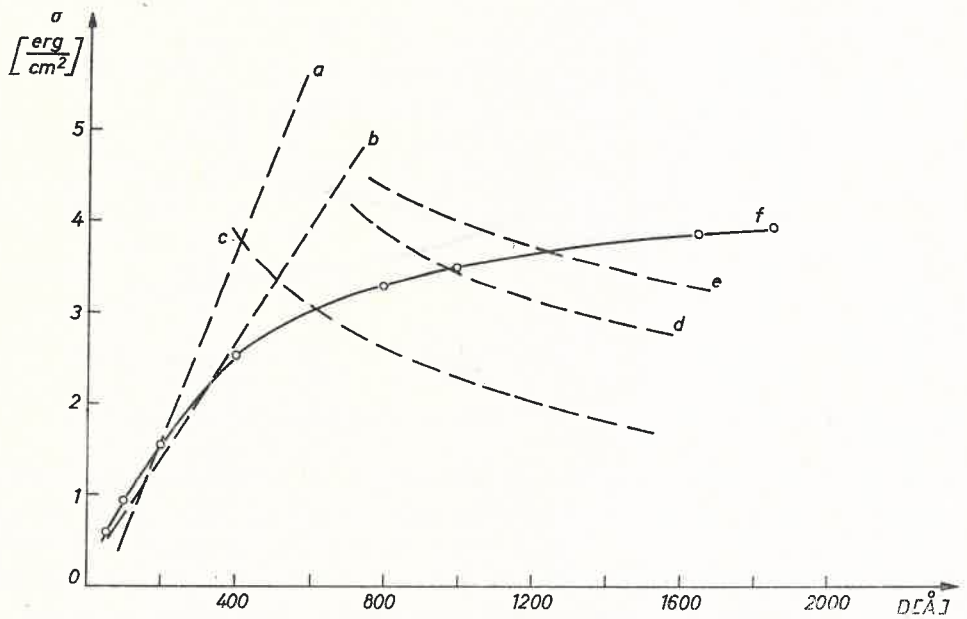

Fig. 7. Energies of Néel, Bloch and cross-tie walls. Néel wall models: a — Feldkeller–Fuchs [8]. b — Aharoni [16]. Bloch wall models: c — LaBonte [17], d — Aharoni [19], e — Brown–LaBonte [18], f — cross-tie wall in our first model

we obtain (Fig. 7) that the cross-tie wall for our first model is energetically favorable for 50 Å $< D <$ 1800 Å. For more complicated models of the Néel walls [8, 16] we obtain that cross-tie wall is energetically favorable for $D > D_1 \approx 200$ Å. For the case of the Bloch wall we obtain the values of the thickness D from 600 Å (for the two dimensional model of LaBonte [17]) to 1400 Å (for the two dimensional model of Brown–LaBonte [18]). As we see this range is different for different wall models but it is in approximate accordance to the experimetal data.

The behaviour of the surface energy density of the cross-tie wall as a function of film thickness for the second model has such character that the model seems to have physical meaning for large values of film thickness ($D \gtrsim 500$ Å). For this range of film thickness we did not obtained correct values for the behaviour of s (D) curve. The behaviour of the Bloch type segments as a function of D is also in contradiction to those foreseen in [8]. On the other hand the presented models yield information on the influence of modification in the description of the Bloch type segments on the most important parameters of the cross-tie wall.

It is possible to make improvements in the theoretical description of such domain walls [2]. One of the most important is to connect the structure of the wall to the complicated material structure of the thin films. On the other hand one should obtain much better results using a two dimensional distribution of magnetization for all fragments of the wall combined with more accurate computations for magnetostatic interaction. Unfortunately such improvements will increase the number of minimization parameters and therefore demand much more computer time.

I wish to express my sincere thanks to dr A. Sukiennicki for numerous valuable discussions.

REFERENCES

[1] M. S. Cohen in *Thin Film Phenomena*, ed. K. Chopra. Mc Graw Hill Comp. 1969.
[2] A. Sukiennicki, J. Strzeszewski, *Acta Phys. Pol.* **A48**, 187 (1975).
[3] S. Middlehoek, *J. Appl. Phys.* **34**, 1054 (1963).
[4] M. Prutton, *Philos. Mag.* **5**, 625 (1960).
[5] A. Aharoni, *J. Appl. Phys.* **37**, 4615 (1966).
[6] N. Minnaja, *J. Phys.* **32** *S*, 406 C–1 (1971).
[7] L. Schwee, J. Watson, *IEEE Trans. Magn.* **9**, 551 (1973).
[8] E. Feldkeller, E. Fuchs, *Z. Angew. Phys.* **18**, 1 (1964).
[9] W. Kayser, *IEEE Trans. Magn.* **3**, 141 (1967).
[10] E. Feldkeller, H. Thomas, *Phys. Kondens. Mater.* **4**, 8 (1965).
[11] H. Bäurich, *Phys. Status Solidi* **23**, K 137 (1967).
[12] S. Middlehoek, *Thesis*, Univ. of Amsterdam 1961.
[13] S. Methfessel, *IBM J. Res. Dev.* **4**, 96 (1960).
[14] P. Hulyer, *Mullard Res. Lab. Rep.* **505**, April (1964).
[15] S. Methfessel et al., *J. Appl. Phys.* **31**, 302 S (1960).
[16] A. Aharoni, *J. Appl. Phys.* **41**, 186 (1970).
[17] A. LaBonte, *J. Appl. Phys.* **40**, 2450 (1969).
[18] W. Brown Jr., A. LaBonte, *J. Appl. Phys.* **36**, 1380 (1965).
[19] A. Aharoni, *Philos. Mag.* **25**, 993 (1970).